

RESEARCH ARTICLE | MAY 06 2024

## Molecular dynamics simulation study of nitrogen vacancy color centers prepared by carbon ion implantation into diamond

Wei Zhao; Zongwei Xu ; Pengfei Wang ; Hanyi Chen

Check for updates

*Nanotechnol. Precis. Eng.* 7, 033007 (2024)

<https://doi.org/10.1063/10.0025756>

View  
Online

Export  
Citation

### Articles You May Be Interested In

Defect evolution and color center generation of high energy density femtosecond laser processed IIa diamond

*Nanotechnol. Precis. Eng.* (April 2025)

Regulation and enhancement of the optical performance of graphene oxide through Ni/Fe/Ag nanoparticles doping

*Nanotechnol. Precis. Eng.* (April 2025)

Germanium-vacancy centers in detonation nanodiamond for all-optical nanoscale thermometry

*Appl. Phys. Lett.* (November 2023)

Nanotechnology and Precision Engineering

纳米技术与精密工程

## Special Topics Open for Submissions

Submit Today!



AIP  
Publishing

# Molecular dynamics simulation study of nitrogen vacancy color centers prepared by carbon ion implantation into diamond

Cite as: Nano. Prec. Eng. 7, 033007 (2024); doi: [10.1063/10.0025756](https://doi.org/10.1063/10.0025756)

Submitted: 11 August 2023 • Accepted: 27 November 2023 •

Published Online: 6 May 2024



[View Online](#)



[Export Citation](#)



[CrossMark](#)

Wei Zhao,<sup>1</sup> Zongwei Xu,<sup>1,a)</sup> Pengfei Wang,<sup>2</sup> and Hanyi Chen<sup>1</sup>

## AFFILIATIONS

<sup>1</sup> State Key Laboratory of Precision Measuring Technology and Instruments, Tianjin University, Tianjin 300072, China

<sup>2</sup> Department of Modern Physics, University of Science and Technology of China, Hefei 230026, China

<sup>a)</sup> Author to whom correspondence should be addressed: [zongweixu@tju.edu.cn](mailto:zongweixu@tju.edu.cn)

## ABSTRACT

Nitrogen vacancy (NV) color centers in diamond have useful applications in quantum sensing and fluorescent marking. They can be generated experimentally by ion implantation, femtosecond lasers, and chemical vapor deposition. However, there is a lack of studies of the yield of NV color centers at the atomic scale. In the molecular dynamics simulations described in this paper, NV color centers are prepared by ion implantation in diamond with pre-doped nitrogen and subsequent annealing. The differences between the yields of NV color centers produced by implantation of carbon (C) and nitrogen (N) ions, respectively, are investigated. It is found that C-ion implantation gives a greater yield of NV color centers and superior location accuracy. The effects of different pre-doping concentrations (400–1500 ppm) and implantation energies (1.0–3.0 keV) on the NV color center yield are analyzed, and it is shown that a pre-doping concentration of 1000 ppm with 2 keV C-ion implantation can produce a 13% yield of NV color centers after 1600 K annealing for 7.4 ns. Finally, a brief comparison of the NV color center identification methods is presented, and it is found that the error rate of an analysis utilizing the identify diamond structure + coordination analysis method is reduced by about 7% compared with conventional identification methods.

© 2024 Author(s). All article content, except where otherwise noted, is licensed under a Creative Commons Attribution (CC BY) license (<https://creativecommons.org/licenses/by/4.0/>). <https://doi.org/10.1063/10.0025756>

## KEYWORDS

NV color center, Ion implantation, Molecular dynamics (MD) simulation, Yield enhancement

## I. INTRODUCTION

Diamond, as an ultrawide-bandgap (5.47 eV) semiconductor, can contain a variety of optical defects, such as nitrogen,<sup>1</sup> silicon,<sup>2</sup> germanium,<sup>3</sup> and magnesium<sup>4</sup> vacancies (NVs, SiVs, GeVs, and MgVs, respectively), and nickel–nitrogen (NE8) defect centers.<sup>5</sup> NV color centers are extensively applied in biofluorescent marking,<sup>6</sup> quantum sensing,<sup>7</sup> nuclear magnetic resonance (NMR),<sup>8</sup> and other techniques owing to their steady luminescence at room temperature and their long spin coherence time. Moreover, the preparation of NV color centers in combination with nanotechnology can be applied to single-photon sources,<sup>9</sup> optical microcavities,<sup>10</sup> and spin-based quantum storage.<sup>8</sup> The current preparation methods for NV color centers involve ion implantation,<sup>11,12</sup> femtosecond

laser processing,<sup>13,14</sup> and chemical vapor deposition (CVD).<sup>15</sup> Experimental preparation of NV<sup>-</sup> color centers can be performed by implanting ions such as protons,<sup>16,17</sup> electrons,<sup>18,19</sup> carbon,<sup>20</sup> nitrogen,<sup>21,22</sup> metal,<sup>23</sup> helium,<sup>24–26</sup> and other noble gases.<sup>27</sup> After ion implantation, a sufficient number of vacancies are formed for the subsequent annealing to promote the combination of vacancies with N atoms to form NV color centers. The conventional ion implantation technique can not only prepare NV color centers with high yield and resolution, but also facilitate the growth of the diamond lattice.<sup>28</sup> In particular, for diamond materials with a high N concentration, NV color centers can be prepared with different depths.<sup>29</sup>

Although NV color center fabrication has been extensively studied experimentally, it has not been clear whether high-yield NV color centers can be reproduced well in simulation studies. However,

high yields of NV color centers are difficult to prepare owing to the required purity. If the diamond substrate material does not contain any N element, the yield of prepared NV color centers is relatively poor and not statistically regular. Lehtinen *et al.*<sup>30</sup> studied the depth distribution and defect evolution of N and Si ions implanted into diamond, but did not present any details of the color center yield. In our previous study,<sup>31</sup> NV color centers were successfully prepared using N-ion implantation by pre-doping the substrate material with N atoms, and the optimal parameters for the preparation were established. However, the high N concentration resulted in an increase in the concentration of paramagnetic defects, which can affect the spin coherence time of NV color centers inside the material and thus degrade sensitivity. Numerous studies have shown that the use of implanted ions other than N atoms can reduce the paramagnetic defects inside the material and facilitate the exploitation of the quantum properties of NV color centers.<sup>19,32</sup> Therefore, the effects of the implanted ions, pre-doping concentration, and implantation energy on the yield of NV color centers needs to be investigated.

In this paper, the NV color center yields from C and N implantation into pre-doped diamond are analyzed using molecular dynamics (MD) simulation, and the results reveal that the NV color centers generated by C-ion implantation are relatively abundant and their positional accuracy is relatively good. The effect of the pre-doping N concentration and the implantation energy on the NV color center yield is then investigated, and NV color centers are successfully obtained with a yield of 13% at an implantation energy of 2 keV. Finally, a preliminary analysis of different NV color center identification methods is conducted, and the results show that the error rate of the identify diamond structure (IDS) + coordination analysis (CA) method can be reduced by about 7% compared with the conventional identification method (IDS + IDS). This detailed study of the preparation of atomic-scale NV color centers provides a theoretical basis for diamond material preparation, defect control, and quantum applications.

## II. EXPERIMENTAL WORK

There are two main methods to create NV color centers. In the first, N ions can be implanted to collide elastically with the C atoms on the original lattice sites and their first nearest neighboring C atoms to knock them away similarly from their previous positions, while the N atoms gradually dissipate kinetic energy and move to the vicinity of the original lattice sites (interstitial sites), creating vacancies in their nearest neighboring positions. Combination of the vacancy and N atoms is then promoted through subsequent annealing to form NV color centers. The second approach is to pre-dope the substrate material with a certain amount of N atoms,<sup>31</sup> replacing some of the C atoms on the original lattice sites inside the diamond substrate material with N atoms in a random manner, and then implanting other ions such as C or N to produce NV color centers. Figure S1 (supplementary material) shows schematics of both methods.

In an MD simulation, the selection of the force field determines the precision of the results. For the interaction between carbon and nitrogen, the Tersoff potential is used, and the short-range interaction is described by the Ziegler–Biersack–Littmark (ZBL)

potential.<sup>33</sup> This approach is based on the Tersoff and ZBL classical potential correction for SiC,<sup>30</sup> which accurately describes the interaction between carbon and silicon.

The diamond substrate material has dimensions of  $142 \times 142 \times 107 \text{ \AA}^3$ , containing 384 000 atoms, and is divided into a Newton layer, a thermostat layer, and a boundary layer. The principal area of investigation is the Newton layer, and the thermostat layer is utilized to dissipate additional kinetic energy and thermal energy. The lattice is equilibrated at 293 K, and periodic boundary conditions are employed in the X and Y directions, while the implantation direction [perpendicular to the (100) plane] is nonperiodic. Relaxation and implantation times are 10 ps and 350 ps, respectively, and the lattice is stabilized by another 150 ps relaxation process after the implantation is complete. It has been shown in previous studies that the most appropriate implantation condition is vertical implantation and 1600 K annealing.<sup>31</sup> Hence, to prevent the appearance of a large number of metastable  $sp^2$ -bonded C atoms, the implantation dose is chosen to be  $10^{14}$  ions/cm<sup>2</sup>. The simulation and visualization post-processing are performed using Large-scale Atomic/Molecular Massively Parallel Simulator (LAMMPS)<sup>34</sup> and OVITO,<sup>35</sup> respectively. See the supplementary material for identification of the NV color centers and for full details of the simulation parameters (Table S1). The mean square displacement (MSD) method to determine the variation tendency of NV color centers. The calculation formula is as follows:

$$\text{MSD} = \frac{1}{N} \sum_{i=1}^N (dx_i^2 + dy_i^2 + dz_i^2), \quad (1)$$

$$D = \frac{1}{2d} \lim_{t \rightarrow \infty} \frac{1}{t} \text{MSD}, \quad (2)$$

where  $N$  is the number of particles,  $dx_i$ ,  $dy_i$ , and  $dz_i$  denote the displacements of atoms in each direction,  $D$  is the self-diffusion coefficient, and  $d = 3$  is the dimension.

## III. RESULTS

### A. Different ion implantations

To produce NV color centers with higher yields and improve the spin coherence time by reducing the quantity of paramagnetic defects (P1) inside the diamond, a comprehensive analysis of two different ion implantations, of C and N, respectively, is performed. On the basis of results in the literature,<sup>31</sup> the annealing temperature is set at 1600 K for 7.4 ns after implantation and the concentration of pre-doped N elements is set at 1000 ppm ( $1.6 \times 10^{21}$  ions/cm<sup>3</sup>). The approximate implantation energies are determined using the stopping and range of ions in matter (SRIM) code<sup>33</sup> by choosing values with similar depth distributions for the two elements. The implantation energies are 1.4 keV and 1.6 keV, respectively (the effect of electron stopping at this energy is negligible, and the percentages of nuclei and electron stopping at different energies can be found in Fig. S2 in the supplementary material). As illustrated in Fig. 1, since the SRIM simulation considers only two-body collisions, there is some discrepancy in the average propagation range when compared with the MD simulation results (where multibody collisions are considered). For N-ion implantation, the entire average penetration depth is relatively shallow, owing to the intense collisions between the incident particles and the shallow C and N atoms of the substrate

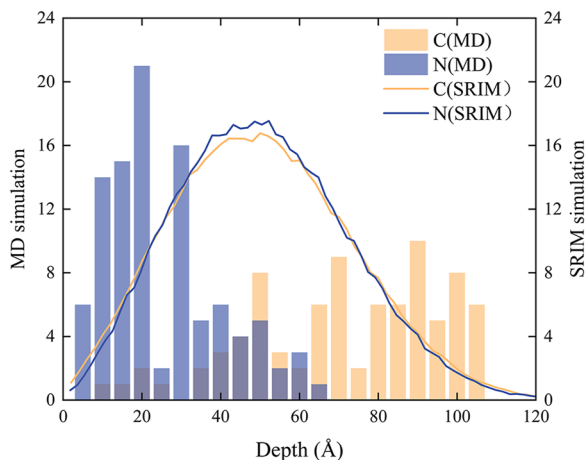


**FIG. 1.** Penetration depths of incident C and N ions according to SRIM and MD simulations.

material, which contributes to a relatively rapid energy dissipation of the incident ions. For C-ion implantation, since the mass of the incident particles is similar to that of the atoms of the substrate material, there are more incident ions that recoil after colliding with the substrate, which makes the interatomic lattice vibrations in the shallow layers of the substrate material more intense. Following the subsequent continuous implantation (along the channel effect direction), the probability of moving along the deep layer gradually increases, resulting in its relatively dispersed and deeper distribution, which is presumably more conducive to the generation of deeper NV color centers.

For convenience in analyzing the differences between NV color centers generated by the two different implanted ions, only the NV color centers generated by pre-doping the substrate material with N atoms are investigated. As shown in Fig. 2, from a comparison of the yields of NV color centers generated by implantation of C and

N ions into diamond, it is found that the number and positional accuracy of NV color centers generated by C-ion implantation are higher than those of NV color centers generated by N-ion implantation for all annealing times, which is consistent with results in the literature.<sup>20</sup> Moreover, according to the model of N-ion implantation into diamond, with continuous transfer of the kinetic energy of the implanted ions, C atoms inside the substrate create vacancies in their vicinity. Through subsequent high-temperature annealing, C vacancies gradually migrate and combine with N atoms to form NV color centers. Therefore, the efficiency of this NV color center formation process is constrained by the number of available vacancies near the stopping positions of N atoms and the cross sections of N-capture vacancies. Besides, the higher the N content, the greater will be the paramagnetic defect concentration inside the substrate material, which affects its spin coherence time as well as the sensitivity of the sensing application. Therefore, by replacing the implanted ions by C ions, not only can the concentration of N ions be appropriately reduced, thus further reducing the content of paramagnetic defects inside the substrate material, but also NV color centers with relatively high yields can be prepared. In addition, since <sup>12</sup>C has a free nuclear spin,<sup>36</sup> the NV color center coherence time will not be limited by the nuclear spin bath, which is beneficial to further enhancement of the spin coherence time of the NV color centers and improved quantum sensing ability.

## B. Influence of pre-doping concentration

Although NV color centers with relatively high yield and positional accuracy have been successfully obtained at a doping concentration of 1000 ppm, the relatively high concentration of P1 centers leads to an increase in the concentration of paramagnetic defects inside the substrate material, which will reduce the spin coherence time of NV color centers and the sensitivity for sensing applications. Therefore, it is necessary to analyze the variation of NV color center yield with pre-doping concentration. The incident particle energy is again chosen to be 1.4 keV, and the concentration of the pre-doped N is 400–1500 ppm.

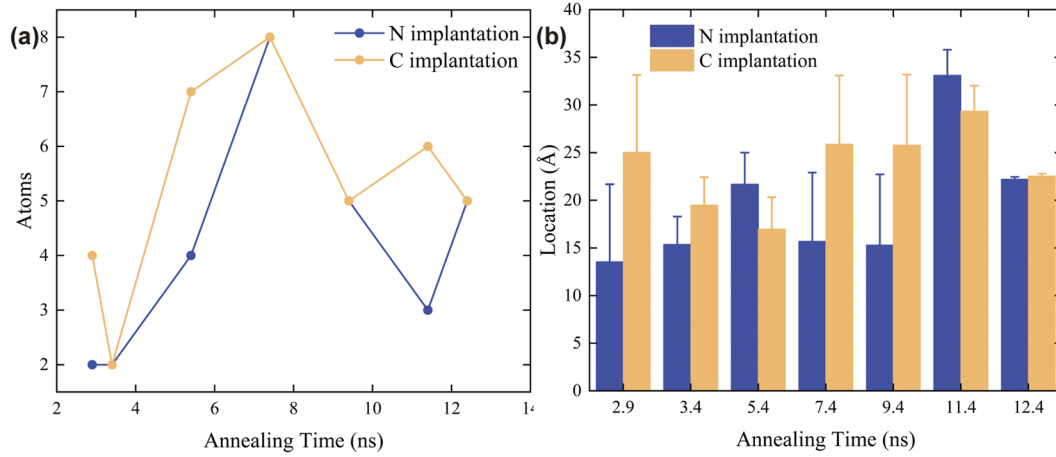


**FIG. 2.** Differences in (a) number and (b) depth distribution of NV color centers at different annealing times for C and N ion-implanted pre-doped diamonds with 1000 ppm N atoms.

**Figures 3(a)** and **3(b)** depict the internal melting point and x-ray diffraction (XRD) results for the substrate material at various doping concentrations before implantation. As the pre-doping concentration rises, the temperature at which the liquid-phase transition of the diamond substrate material occurs is basically the same, about 8500 K, as shown in **Fig. 3(a)**. The difference is primarily manifested by the increasing potential energy and pressure inside the lattice during the solid–liquid phase transition. The outcome of the XRD analysis of the C1–C9 samples before implantation according to the MD simulation is shown in **Fig. 3(b)**, where three characteristic diffraction peaks of diamond, namely, (111), (220), and (311), can be clearly observed in all samples, corresponding to values of 43.8°, 75.4°, and 91.0°, which are consistent with the experimentally obtained results.<sup>37</sup> It is also observed that as the amount of pre-doped N increases, the intensities of the diamond XRD peaks exhibit less variation. When the doping concentration is more than 1000 ppm, there is likewise no noticeable modification of the spreading of the characteristic diffraction peaks of diamond. However, the characteristic peaks gradually appear to broaden, presumably owing to the presence of C–N bonds (n-type doping) resulting in a slightly expanded lattice, which causes a minor alteration in the quality of the diamond substrate lattice and promotes the generation of vacancies and interstitials.<sup>32</sup>

The MSD is shown in **Fig. 3(c)** as a function of implantation time for different pre-doping concentrations (further details of the variations during the whole implantation process can be found in Fig. S3 in the supplementary material). The MSD method is able to describe the melting point variation within the system as well as determining the self-diffusion coefficient of the lattice.<sup>38</sup>

It is obvious from **Figs. 3(d)–3(f)** that the increase in yield of NV color centers is not linear in the pre-doping concentration. The numbers of NV color centers produced at doping concentrations of 400–900 ppm are consistently lower, maintaining a yield of 1%–4%, and the yield fluctuates randomly with concentration; likewise, with a further increase in the pre-doping concentration (>1000 ppm), there is no obvious increase in yield. According to **Table I**, if the self-diffusion coefficient is around  $1 \times 10^{-4}$ , then a significant amount of NV color centers will be generated. When the self-diffusion coefficient is higher than this value, owing to the relatively high potential energy of the atoms around the originally formed NV color centers, there is greater transfer of thermal vibrations to the NV color centers, facilitating the dissociation of the latter due to temperature changes, and enhancing the creation of double vacancies. The self-diffusion coefficient of the atoms inside the entire lattice is weak when the self-diffusion coefficient is  $<1 \times 10^{-4}$ , decreasing the transfer of thermal vibrations to the interstitial N atoms and reducing

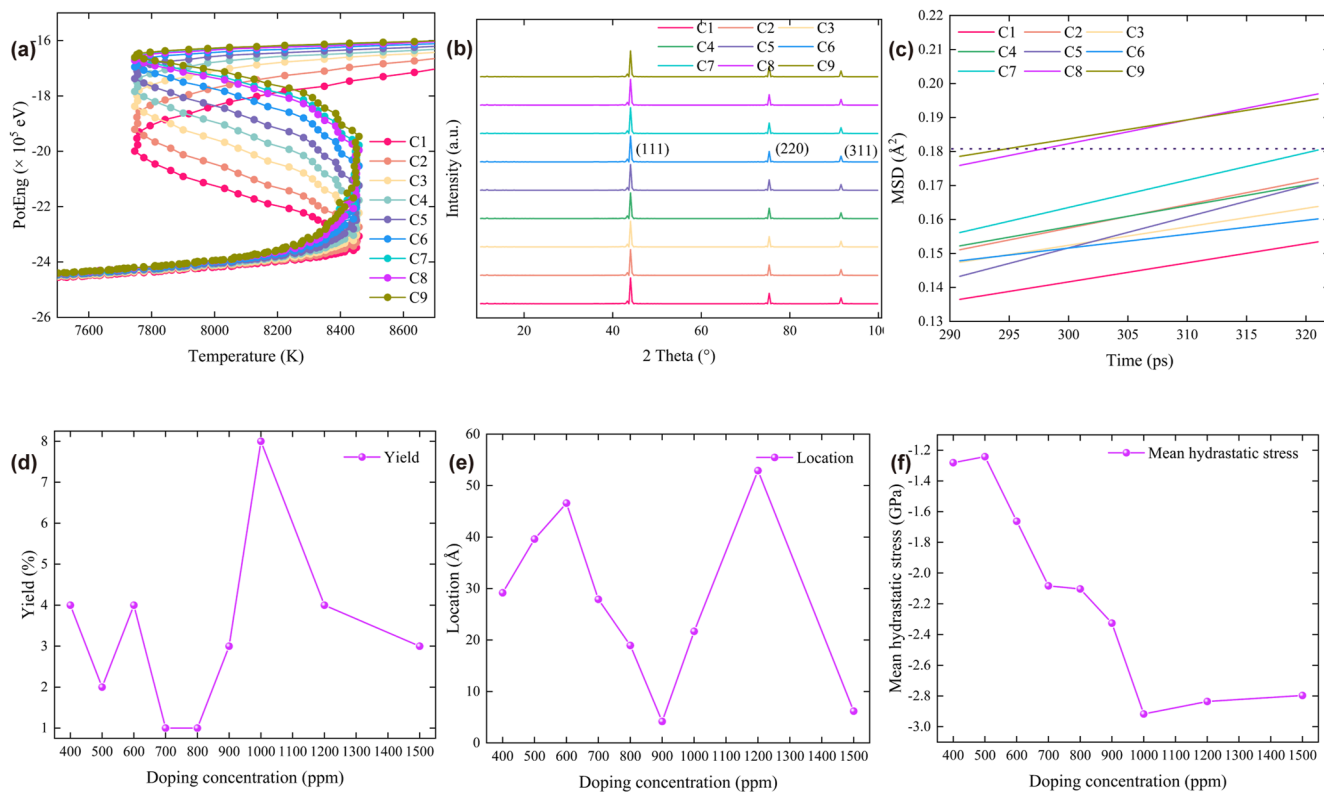


**FIG. 3.** (a) Variation of diamond melting point, (b) XRD, (c) MSD, (d) NV color center yield, (e) positional location, and (f) mean hydrostatic stress of the lattice at various doping concentrations C1–C9 (see **Table I**). The MSD analysis is in the linear variation region at the implantation stage. The NV color center yield and positional accuracy are the results after annealing at 1600 K and 7.4 ns. The mean hydrostatic stress is in the relaxation stage after the completion of implantation.

**TABLE I.** Coefficients of linear expression obtained by MSD fitting at different doping concentrations.  $a$  is the truncation and  $b$  is the slope.  $R^2$  is the correlation coefficient.

Pre-doping concentration (ppm)		$a$	$b (\times 10^{-4})$	$R^2$
400	(C1)	-0.026 55	5.6068	0.783 46
500	(C2)	-0.050 73	6.939 95	0.7845
600	(C3)	-0.010 57	5.4327	0.703 48
700	(C4)	-0.026 56	6.148	0.507 92
800	(C5)	-0.122 22	9.129 19	0.814 92
900	(C6)	0.029 11	4.083 04	0.576 54
1000	(C7)	-0.077 68	8.040 35	0.728 94
1200	(C8)	-0.026 86	6.971 87	0.462 53
1500	(C9)	0.015 72	5.5993	0.777 16

the NV color center yield. Analysis of the mean hydrostatic stress inside the system reveals that in the pre-doped system at 500 ppm, the internal compressive stress of the material decreases, and the yield rate decreases significantly, after which, with a further rise in pressure, the yield increases slightly. However, the color center yield basically remains unchanged when the pressure changes by less than 0.2 GPa. At pre-doping concentrations higher than 1000 ppm, the pressure in the interior of the material is further diminished. With regard to the depth distribution of the color centers, it is found that the penetration depth is relatively close to the surface in samples with pre-doping concentration below 1000 ppm and comparatively low yield, and the structural stability and optical properties of these samples are inferior,<sup>39</sup> which is not conducive to exploitation of quantum properties. The generation of shallow NV color centers is mostly caused by partial imperfections of the lattice surface and unregulated formation of defect clusters.<sup>40</sup> Further detailed analysis may require the use of different potentials in the MD simulations<sup>41</sup>. One possible solution to the problem of shallow NV color centers is the use of swift heavy ions to facilitate implantation.<sup>42</sup>

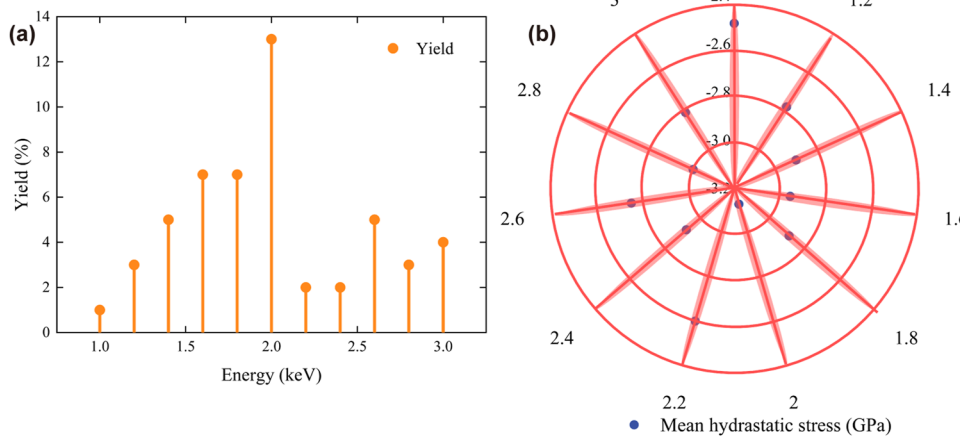


**FIG. 4.** Variations of (a) color center yield and (b) mean hydrostatic stress with implantation energy (the range of stress values is from -2.4 to 3.2, and the range of implantation energy is from 1 to 3).

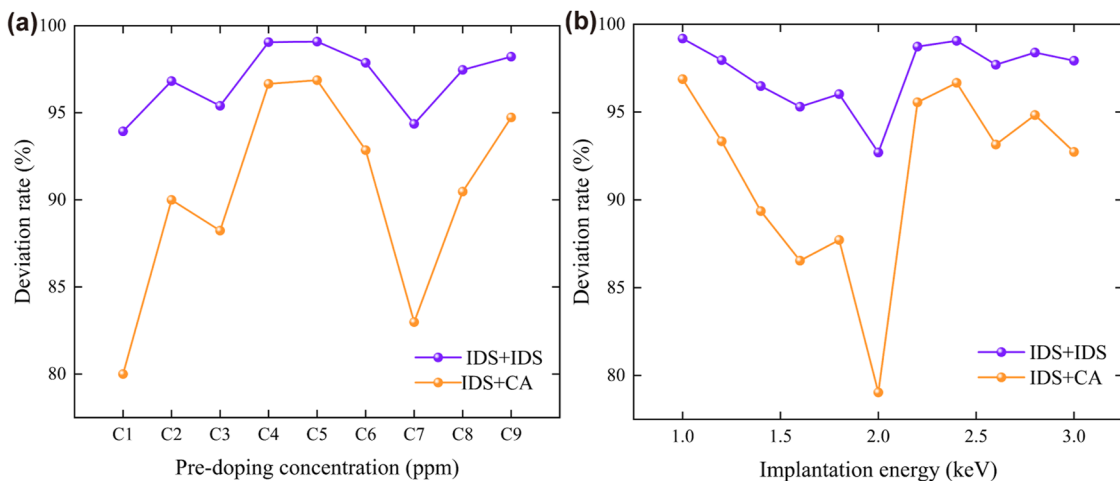
### C. Effect of implantation energy

Figure 4(a) shows the variation in NV color center yield with implantation energy. The specific velocities used in the MD simulations are listed in Table S2 (supplementary material). It can be seen that from 1.0 eV to 2.0 keV energy, the NV color center yield gradually increases and peaks with a value of about 13% at 2.0 keV, drops again at 2.2 keV, and then increases, although it does not exceed 5%. A possible explanation of this behavior is as follows. As the implantation energy increases, the probability of cascade collisions near the surface increases, which can lead to the reappearance of off-site collisions around the previously generated NV color centers, resulting in the formation of more complex structures, such as the appearance of off-site atoms of C at the next nearest neighbors of N, which contributes to the destruction of the NV color center structure. Another possible reason is that with further increases in implantation energy, more defect clusters are formed inside the substrate after C-ion implantation, and after high-temperature annealing recovery, the defect clusters undergo thermal dissociation to form compound defects.<sup>43</sup>

The trend of variation of NV color center yield can be further illustrated by investigating the stress variations inside the lattice after completion of implantation. Figure 4(b) displays the mean hydrostatic stress change inside the system after completion of implantation and subsequent relaxation. It is evident that the compressive stress inside the lattice reaches a maximum (-3.2 GPa) for 2.0 keV implantation. Through the subsequent annealing recovery process, compressive strain is gradually released, which is beneficial for the generation of more NV color centers. Thus, a comprehensive analysis shows that under low-energy implantation conditions, 2 keV C atoms vertically implanted in diamond can provide higher yields of NV color centers, which helps to provide a theoretical reference for the selection of macroscopic experimental parameters.

### D. Error rate

The error rates of the two methods of NV color center identification (IDS + IDS and IDS + CA) before accurate location



**FIG. 5.** Error rates in identification of NV color centers by two methods for different doping concentrations (a) and implantation energies (b).

observation are analyzed in Fig. 5, from which it can be concluded that the error rates of the two identification methods decrease gradually with increasing NV color center yield, while the overall NV color center identification error rate from the IDS + CA method is relatively low (the error rate is reduced by 7% on average compared with the IDS method). However, the error rates of both methods still remain above 80%. The errors originate primarily because when the methods are used for identification, only the bonding structure around the N atoms can be identified, and the existence of vacancies in the first nearest neighbors of vacancies (e.g., di-vacancies) cannot be excluded. Furthermore, the presence of clusters also increases the error rate of identification, owing to incomplete recovery from lattice damage after annealing. The reason for the relatively large error of the IDS method is that during the relaxation phase after implantation and annealing, the system gradually attains a steady state and certain lattice vibrations (shrinkage and expansion) exist. The bond lengths of the atoms in the system will be fluctuating at this time. However, the IDS command cannot accurately adjust the bond lengths used for identification, with the result that a large number of interstitial N atoms are identified as NV color centers. In the case of the IDS + CA identification method, the main error originates from the fact that when IDS + CA is used to analyze a system in which the first nearest neighbor of an N atom is also an N atom, or in which two N atoms are bonded to the same vacancy, an NV color center will also be recognized mistakenly. Further combinations of other methods are necessary to improve the efficiency of NV color center identification.

#### IV. CONCLUSIONS

MD simulations of NV color centers fabricated in diamond by ion implantation have been performed. By random pre-doping of the lattice with N, NV color centers have been successfully generated with high yield. Comparison of the numbers of NV color centers that can be prepared by C and N ions, respectively, at similar penetration depths shows that under the same implantation and annealing conditions (except for the implantation energy), C-ion implantation

produces a larger number of NV color centers, and these are located with a higher accuracy.

The effect of the pre-doped N concentration on the NV color center yield has been analyzed, and it has been found that an increase in the pre-doped concentration does not lead to a linear variation in the number of NV color centers, and that when the doping concentration is higher than 1000 ppm, there is a further decrease in the NV color center yield, accompanied by a high content of paramagnetic defects within the lattice.

The trend of variation of the number of NV color centers with implantation energy for low-energy C-ion implantation into diamond has been studied. The yield of NV color centers peaks at a value of 13% for an implantation energy of 2 keV, which is due to the relatively high compressive stress in the system under these conditions, and the stress relief caused by annealing makes the N atoms in the interstitial sites move to the lattice sites and combine with the vacancies to form NV color centers.

Finally, the error rates of two methods for identifying NV color centers have been investigated, and it has been shown that the IDS + CA method can reduce the error rate by 7%, but the error caused by double vacancies cannot be eliminated, although the error rate could be reduced by using a different potential to further enhance the yield of NV color centers.

In summary, the MD simulations of yield enhancement of NV color centers at the microscopic scale presented here can provide a theoretical basis for the development of practical quantum applications.

#### SUPPLEMENTARY MATERIAL

See supplementary material for more information about pre-doping MD simulation setup for the fabrication of NV color centers.

#### ACKNOWLEDGMENTS

This research was supported by the National Natural Science Foundation of China (Grant Nos. 52035009 and 51761135106),

the State Key Laboratory of Precision Measuring Technology and Instruments (Pilt1705), the Henan Key Laboratory of Intelligent Manufacturing Equipment Integration for Superhard Materials (JDKJ2022-01), and the “111” project by the State Administration of Foreign Experts Affairs and the Ministry of Education of China (Grant No. B07014).

## AUTHOR DECLARATIONS

### Conflict of Interest

The authors have no conflicts to disclose.

## DATA AVAILABILITY

The data that support the findings of this study are available within the article.

## REFERENCES

- <sup>1</sup>Rabeau JR, Rechart P, Tamanyan G, et al. Implantation of labelled single nitrogen vacancy centers in diamond using <sup>15</sup>N. *Appl Phys Lett* 2006;88(2):023113. <https://doi.org/10.1063/1.2158700>.
- <sup>2</sup>Zhang Y, Wang K, Ding S, Tian Y, et al. Photoluminescence studies of nitrogen-vacancy and silicon-vacancy centers transformation in CVD diamond. *J Phys Condens Matter* 2020;32(34):34LT01. <https://doi.org/10.1088/1361-648x/ab8987>.
- <sup>3</sup>Zaghrioui M, Agafonov VN, Davydov VA. Nitrogen and group-IV (Si, Ge) vacancy color centres in nano-diamonds: Photoluminescence study at high temperature (25 °C–600 °C). *Mater Res Express* 2020;7(1):015043. <https://doi.org/10.1088/2053-1591/ab6647>.
- <sup>4</sup>Corte E, Andrini G, Nieto Hernandez E, et al. Magnesium-vacancy optical centers in diamond. *ACS Photonics* 2023;10(1):101–110. <https://doi.org/10.1021/acspophotonics.2c01130>.
- <sup>5</sup>Rabeau JR, Chin YL, Prawer S, et al. Fabrication of single nickel-nitrogen defects in diamond by chemical vapor deposition. *Appl Phys Lett* 2005;86(13):131926. <https://doi.org/10.1063/1.1896088>.
- <sup>6</sup>Liu W, Naydenov B, Chakrabortty S, et al. Fluorescent nanodiamond-gold hybrid particles for multimodal optical and electron microscopy cellular imaging. *Nano Lett* 2016;16(10):6236–6244. <https://doi.org/10.1021/acs.nanolett.6b02456>.
- <sup>7</sup>Acosta VM, Jensen K, Santori C, et al. Electromagnetically induced transparency in a diamond spin ensemble enables all-optical electromagnetic field sensing. *Phys Rev Lett* 2013;10(21):213605. <https://doi.org/10.1103/physrevlett.110.213605>.
- <sup>8</sup>Pezzagna S, Meijer J. Quantum computer based on color centers in diamond. *Appl Phys Rev* 2021;8(1):011308. <https://doi.org/10.1063/5.0007444>.
- <sup>9</sup>Bulu I, Babinec T, Hausmann B, et al. Plasmonic resonators for enhanced diamond NV-center single photon sources. *Opt Express* 2011;19(6):5268–5276. <https://doi.org/10.1364/oe.19.005268>.
- <sup>10</sup>Larsson M, Dinyari KN, Wang H. Composite optical microcavity of diamond nanopillar and silica microsphere. *Nano Lett* 2009;9(4):1447–1450. <https://doi.org/10.1021/nl8032944>.
- <sup>11</sup>Chu Y, de Leon NP, Shields BJ, et al. Coherent optical transitions in implanted nitrogen vacancy centers. *Nano Lett* 2014;14(4):1982–1986. <https://doi.org/10.1021/nl404836p>.
- <sup>12</sup>K. Ohno, F. Joseph Heremans, L. C. Bassett, et al. Engineering shallow spins in diamond with nitrogen delta-doping. *Appl Phys Lett* 2012;101(8):082413. <https://doi.org/10.1063/1.4748280>.
- <sup>13</sup>Fujiwara M, Inoue S, Masuno S-i, et al. Creation of NV centers over a millimeter-sized region by intense single-shot ultrashort laser irradiation. *APL Photonics* 2023;8(3):036108. <https://doi.org/10.1063/5.0137093>.
- <sup>14</sup>Chen Y-C, Salter PS, Knauer S, et al. Laser writing of coherent colour centres in diamond. *Nat Photonics* 2016;11(2):77–80. <https://doi.org/10.1038/nphoton.2016.234>.
- <sup>15</sup>Chakraborty T, Lehmann F, Zhang J, et al. CVD growth of ultrapure diamond, generation of NV centers by ion implantation, and their spectroscopic characterization for quantum technological applications. *Phys Rev Mater* 2019;3(6):065205. <https://doi.org/10.1103/physrevmaterials.3.065205>.
- <sup>16</sup>Mrozek M, Schabikowski M, Mitura-Nowak M, et al. Nitrogen-vacancy color centers created by proton implantation in a diamond. *Materials* 2021;14(4):833. <https://doi.org/10.3390/ma14040833>.
- <sup>17</sup>Jin H, Bettoli AA. Influence of thermal annealing on the properties of proton implanted diamond waveguides. *Carbon* 2021;171:560–567. <https://doi.org/10.1016/j.carbon.2020.09.009>.
- <sup>18</sup>Guo R, Wang K, Zhang Y, et al. Adjustable charge states of nitrogen-vacancy centers in low-nitrogen diamond after electron irradiation and subsequent annealing. *Appl Phys Lett* 2020;117(17):172104. <https://doi.org/10.1063/5.0023369>.
- <sup>19</sup>Zhang C, Yuan H, Zhang N, et al. Dependence of high density nitrogen-vacancy center ensemble coherence on electron irradiation doses and annealing time. *J Phys D Appl Phys* 2017;50(50):505104. <https://doi.org/10.1088/1361-6463/aa97b3>.
- <sup>20</sup>Ohno K, Joseph Heremans F, de las Casas CF, et al. Three-dimensional localization of spins in diamond using <sup>12</sup>C implantation. *Appl Phys Lett* 2014;105(5):052406. <https://doi.org/10.1063/1.4890613>.
- <sup>21</sup>van Dam SB, Walsh M, Degen MJ, et al. Optical coherence of diamond nitrogen-vacancy centers formed by ion implantation and annealing. *Phys Rev B* 2019;99(16):161203. <https://doi.org/10.1103/physrevb.99.161203>.
- <sup>22</sup>Feng F, Zhang W, Zhang J, et al. Optimizing the density of nitrogen implantation for generating high-density NV center ensembles for quantum sensing. *Eur Phys J D* 2019;73(9):202. <https://doi.org/10.1140/epjd/e2019-100047-8>.
- <sup>23</sup>Santori C, Barclay PE, Fu K-MC, Beausoleil RG. Vertical distribution of nitrogen-vacancy centers in diamond formed by ion implantation and annealing. *Phys Rev B* 2009;79(12):125313. <https://doi.org/10.1103/physrevb.79.125313>.
- <sup>24</sup>Kleinsasser EE, Stanfield MM, Banks JKQ, et al. High density nitrogen-vacancy sensing surface created via He<sup>+</sup> ion implantation of <sup>12</sup>C diamond. *Appl Phys Lett* 2016;108(20):202401. <https://doi.org/10.1063/1.4949357>.
- <sup>25</sup>Huang Z, Li WD, Santori C, et al. Diamond nitrogen-vacancy centers created by scanning focused helium ion beam and annealing. *Appl Phys Lett* 2013;103(8):081906. <https://doi.org/10.1063/1.4819339>.
- <sup>26</sup>Sumikura H, Hirama K, Nishiguchi K, et al. Highly nitrogen-vacancy doped diamond nanostructures fabricated by ion implantation and optimum annealing. *APL Mater* 2020;8(3):031113. <https://doi.org/10.1063/5.0001922>.
- <sup>27</sup>Räcke P, Pietzonka L, Meijer J, et al. Vacancy diffusion and nitrogen-vacancy center formation near the diamond surface. *Appl Phys Lett* 2021;118(20):204003. <https://doi.org/10.1063/5.0046031>.
- <sup>28</sup>Kalish R, Reznik A, Prawer S, et al. Ion-implantation-induced defects in diamond and their annealing: Experiment and simulation. *Phys Status Solidi A* 1999;174(1):83–99. [https://doi.org/10.1002/\(sici\)1521-396x\(199907\)174:1%3c83::aid-pssa83%3e3.0.co;2-3](https://doi.org/10.1002/(sici)1521-396x(199907)174:1%3c83::aid-pssa83%3e3.0.co;2-3).
- <sup>29</sup>Chen L, Miao X, Ma H, et al. Synthesis and characterization of diamonds with different nitrogen concentrations under high pressure and high temperature conditions. *CrystEngComm* 2018;20(44):7164–7169. <https://doi.org/10.1039/c8ce01533c>.
- <sup>30</sup>Lehtinen O, Naydenov B, Börner P, et al. Molecular dynamics simulations of shallow nitrogen and silicon implantation into diamond. *Phys Rev B* 2016;93(3):035202. <https://doi.org/10.1103/physrevb.93.035202>.
- <sup>31</sup>Zhao W, Xu Z, Ren F, et al. Enhancing the fabrication yield of NV centers in diamond by pre-doping using molecular dynamics simulation. *Diamond Relat Mater* 2023;132:109683. <https://doi.org/10.1016/j.diamond.2023.109683>.
- <sup>32</sup>Watanabe A, Nishikawa T, Kato H, et al. Shallow NV centers augmented by exploiting n-type diamond. *Carbon* 2021;178:294–300. <https://doi.org/10.1016/j.carbon.2021.03.010>.

- <sup>33</sup>Ziegler JF, Biersack JP. The stopping and range of ions in matter. Treatise on Heavy-Ion Science: Springer. 1985. pp. 93–129.
- <sup>34</sup>Plimpton S. Fast parallel algorithms for short-range molecular dynamics. *J Comput Phys* 1995;117(1):1–19. <https://doi.org/10.1006/jcph.1995.1039>.
- <sup>35</sup>Stukowski A. Visualization and analysis of atomistic simulation data with OVITO—The open visualization tool. *Modell Simul Mater Sci Eng* 2010;18(1):015012. <https://doi.org/10.1088/0965-0393/18/1/015012>.
- <sup>36</sup>Balasubramanian G, Neumann P, Twitchen D, et al. Ultralong spin coherence time in isotopically engineered diamond. *Nat Mater* 2009;8(5):383–387. <https://doi.org/10.1038/nmat2420>.
- <sup>37</sup>Pang H, Wang X, Zhang G, et al. Characterization of diamond-like carbon films by SEM, XRD and Raman spectroscopy. *Appl Surf Sci* 2010;256(21):6403–6407. <https://doi.org/10.1016/j.apsusc.2010.04.025>.
- <sup>38</sup>Yan X, Feng Y, Qiu L, Zhang X. Thermal conductivity and phase change characteristics of hierarchical porous diamond/erythritol composite phase change materials. *Energy* 2021;233:121158. <https://doi.org/10.1016/j.energy.2021.121158>.
- <sup>39</sup>Neethirajan JN, Hache T, Paone D, et al. Controlled surface modification to revive shallow NV<sup>-</sup> centers. *Nano Lett* 2023;23(7):2563–2569. <https://doi.org/10.1021/acs.nanolett.2c04733>.
- <sup>40</sup>Janitz E, Herb K, Volker LA, et al. Diamond surface engineering for molecular sensing with nitrogen-vacancy centers. *J Mater Chem C* 2022;10(37):13533–13569. <https://doi.org/10.1039/d2tc01258h>.
- <sup>41</sup>Buchan JT, Robinson M, Christie HJ, et al. Molecular dynamics simulation of radiation damage cascades in diamond. *J Appl Phys* 2015;117(24):245901. <https://doi.org/10.1063/1.4922457>.
- <sup>42</sup>Lake RE, Persaud A, Christian C, et al. Direct formation of nitrogen-vacancy centers in nitrogen doped diamond along the trajectories of swift heavy ions. *Appl Phys Lett* 2021;118(8):084002. <https://doi.org/10.1063/5.0036643>.
- <sup>43</sup>Lümann T, Raatz N, John R, et al. Screening and engineering of colour centres in diamond. *J Phys D Appl Phys* 2018;51(48):483002. <https://doi.org/10.1088/1361-6463/aadfab>.



**Zongwei Xu** is a Professor at Tianjin University and a Doctoral Supervisor. His research interests include ultrafast energy beam (ion and laser) processing, Raman and photoluminescence spectroscopy characterization, wide-bandgap semiconductor devices, microcutting tools, and nanocutting technology. He is the Chairman of the First Sino-German Symposium on Defect Engineering in SiC Device Manufacturing—Atomistic Simulations, Characterization and Processing, and the Principal Investigator of the 2021–2023 Mobility Programme of the Sino-German Center for Research Promotion (M-0396).



**Pengfei Wang** is currently Associate Professor in the Department of Modern Physics at the University of Science and Technology of China, Hefei, China. He received his B.S. in Physics from Jilin University (China) in 2008 and his Ph.D. in Quantum Information Physics in 2015. His research interests are quantum sensing and nanoscale magnetic resonance imaging based on nitrogen vacancy center in diamond.



**Hanyi Chen**, a native of Changsha, Hunan Province, is an undergraduate student at Tianjin University. His interest is quantum communication.



**Wei Zhao** is at the State Key Laboratory of Precision Measuring Technology and Instruments, School of Precision Instruments and Optoelectronics Engineering, Tianjin University. He is studying for his Master's degree. His research interest includes molecular dynamics simulations and processing of diamonds using femtosecond lasers.